International Journal of High Speed Electronics and Systems
Vol. 25, Nos. 3 & 4 (2016) 1640023 (8 pages)

DOI: 10.1142/S0129156416400231

Intensive Terahertz Radiation from $In_XGa_{1-X}As$ due to Photo-Dember Effect

Dmitry S. Ponomarev*, Rustam A. Khabibullin, Aleksandr E. Yachmenev, and Petr P. Maltsev†

Institute of Ultra High Frequency Semiconductor Electronics of RAS, Moscow, 117105, Russia
**ponomarev_dmitr@mail.ru*
†iuhfseras2010@yandex.ru

Igor E. Ilyakov, Boris V. Shiskin, and Rinat A. Akhmedzhanov

Institute of Applied Physics of RAS, Nizhny Novgorod, 603950, Russia

Received 03 October 2016
Accepted 14 November 2016

We have proposed and investigated $In_yGa_{1-y}As$ photoconductor grown by molecular-beam epitaxy on low-temperature step-graded metamorphic buffer. It exhibits superior bandwidth up to 6 THz and provides optical-to-terahertz conversion efficiency up to ~ 10^{-5} for rather low optical fluence ~ 40 μJ/cm^2. The intensity of THz generation for the given structure is two orders higher than for low-temperature grown GaAs due substantial contribution of photo-Dember effect.

Keywords: InGaAs; photo-Dember effect; THz radiation; molecular-beam epitaxy; optical-to-terahertz conversion efficiency; metamorphic buffer; time-domain spectroscopy.

1. Introduction

Terahertz (THz) technology has become increasingly popular due to its unique applications in security screening, space exploration, biological sensing and medical imaging.[1,2] Among various techniques for THz generation, photoconductive devices have demonstrated very promising performance for generating both pulsed and continuous-wave THz radiation. THz time-domain spectroscopy (THz-TDS) is widely used in materials science, biology and medicine for investigation of molecules, DNK, RNK, cancer tumors, proteins, etc. THz sources that are used in THz-TDS can be divided into two groups. The first one is attributed to nonlinear conversion of femtosecond laser radiation, and the second is connected with ultrafast dynamics of photoexcited carriers in semiconductors - the so-called photoconductive emitters that use SI-GaAs,[3] low-temperature grown GaAs (LT GaAs)[4,5] and also $In_xGa_{1-x}As$ as a photoconductive material.

$In_xGa_{1-x}As$ is an attractive candidate for emission of THz radiation at optical pump 1.0–1.6 μm[6,7] where SI or LT GaAs do not work. An ultrafast optical pulse with photon energy above the semiconductor band-gap strikes the semiconductor and creates electron-hole pairs at subsurface of the semiconductor. These pairs are rapidly accelerated by the built-in electric field resulting in a radiative dipole parallel to surface normal.[8,9] The most common used photoconductive THz emitter is photoconductive antenna (PCA) where photoexcited carries are accelerated by applied external bias.[10,11] Large external biases are essential to increase the power spectrum of PCA thus the photoconductive material has to be high resistive. Initially $In_xGa_{1-x}As$ has low resistivity and suffers from high dark currents which are detrimental for biased photoconductive devices. There were many attempts to improve it, for instance different authors proposed ErAs islands incorporated into InAlAs/InGaAs quantum wells,[9,10] Be-doped LT InGaAs,[11] ion-implantation in InGaAs[12,13] and etc.

THz generation may occur without an external electrical bias as a result of the boundary conditions on the carrier transport within a semiconductor as a result of the photo-Dember (PD) effect.[14,15] The mechanism of PD effect arises from the differing diffusion mobilities of holes and electrons within a semiconductor. As a rule electron mobility is higher than hole mobility thus under ultrafast optical excitation the spatial distribution of electron-hole pairs occurs leading to THz radiation. PD effect better occurs in narrow-band semiconductors where the difference between electron and hole mobilities is much stronger, for instance in InAs and InN.[16-18] In thermal equilibrium the ratio of the mobilities of electrons in the Γ-valley and heavy holes for $In_xGa_{1-x}As$ ($x \geq 0.4$) is about 40 and less than 20 for LT GaAs.[19] Thus $In_xGa_{1-x}As$ can be used as promising candidate in PD emitters for broadband THz generation. It is important to note that in case of PD effect there is no need of high resistivity of $In_xGa_{1-x}As$ and THz emission can scale with the excitation area by multiplexing (repeating) the number of emitters on a wafer.[20,21] In Ref. 19 it was shown that PD emitters provide even higher bandwidth than photoconductive emitters.

The aim of present work is the development of growth technique and investigation of $In_{0.38}Ga_{0.62}As$ photoconductive material where THz generation is achieved by two mechanisms: 1) acceleration of the photoexcited carriers by the built-in electric field and 2) by PD effect. Due to there is no lattice-matched wafers to $In_xGa_{1-x}As$ ($0 < x < 0.4$) we have proposed the step-graded metamorphic buffer (MB) which allows stoichiometric epitaxial growth of $In_{0.38}Ga_{0.62}As$ on GaAs wafer.

2. The Samples and Experimental Setup

The sample of $In_{0.38}Ga_{0.62}As$ was grown by molecular-beam epitaxy (MBE) on (100) GaAs wafer. Its schematic diagram is shown in Fig. 1. The growth temperature of the photoconductive layer $In_{0.38}Ga_{0.62}As$ was set up to 490 ºC and then reduced to 400 ºC when MB was grown. The step-graded 1.0 μm MB with inverse step $In_{0.38}Al_{0.62}As$ consists of seven $In_xAl_{1-x}As$ layers with x increasing from 0.1 to 0.46. The idea of the given buffer is in step-by-step adjusting of the crystalline parameters of photoconductive layer and GaAs wafer.[22] The inverse step with low indium content decreases elastic strain in the active (photoconductive) area and improves it's structural property.[23,24] The post-growth annealing for $In_{0.38}Ga_{0.62}As$ grown without access arsenic pressure is no need to be carried out.

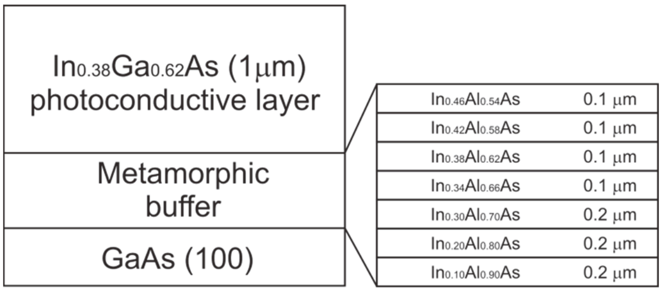

Fig. 1. Schematic diagram of $In_{0.38}Ga_{0.62}As$ photoconductor grown on step-graded metamorphic buffer.

For comparison we also grew and investigated LT GaAs with heavily doped n-GaAs buffer layer. Previously[5] we have shown that LT GaAs grown by MBE with several thin δ-Si doped layers embedded into the photoconductive layer GaAs exhibits picosecond carrier lifetimes. Authors in Ref. 25 showed that use of additional n-GaAs layer beneath LT GaAs enhances built-in electric field on the interface photoconductive layer/buffer layer and thus increase radiated THz electric field. The growth temperature of LT GaAs was set up to 215 ºC. The post-growth annealing was carried out *in situ* at 600 ºC during 20 min.

The structural properties were investigated by means of high resolution double crystal X-ray diffraction. Diffraction rocking curves (DRC) were measured on Rigaku Ultima IV.

The samples were investigated and compared by conventional THz-TDS system. They were irradiated by Ti:sapphire mode-locked laser pulses with 795 nm central wavelength and 50 fs pulse duration (pulse energy 800 μJ, aperture 7.0 mm. The generated THz pulses were focused by an off-axis parabolic mirror on a detection crystal [(100) cut 200 μm GaP crystal] and THz electric field was measured by a standard ellipsometric scheme.[26] Carrier lifetimes were measured by using a time-resolved pump-probe technique.

3. Results and Discussion

Figure 2 depicts DRC for $In_{0.38}Ga_{0.62}As$ measured in θ/2θ-scanning mode (θ is the angle between the reflecting plane and the incident beam, 2θ is the angle between the incident and reflected X-ray beams). It allows determination of the lattice parameters in various directions by the angular positions of peaks on DRC. For symmetric reflections we chose (400) plane.

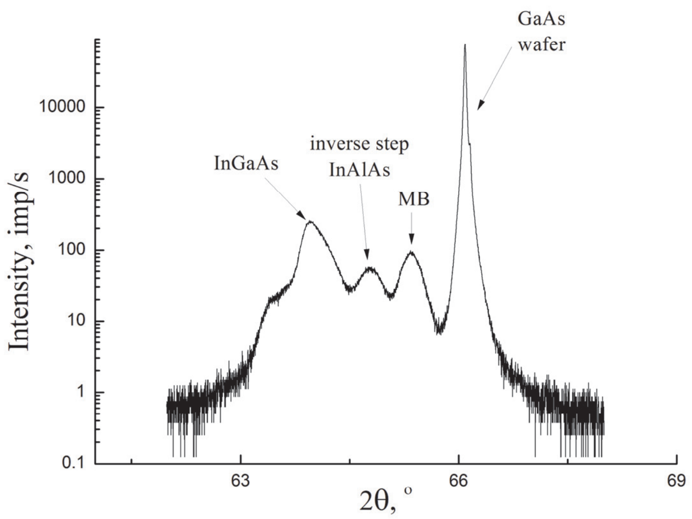

Fig. 2. Diffraction rocking curve of $In_{0.38}Ga_{0.62}As$ grown on step-graded metamorphic buffer.

As seen in Fig. 2 right sharp peak corresponds to (100) GaAs while the left one to photoconductive layer $In_{0.38}Ga_{0.62}As$. Two peaks between them relate to MB and inverse step $In_{0.38}Al_{0.62}As$. We used asymmetric (411) reflections to extract in-plane and out-of-plane lattice parameters for $In_{0.38}Ga_{0.62}As$ (5.8010 Å and 5.8211 Å respectively) and after we calculated the deformation of the given layer that was estimated as $\varepsilon_{res} \sim 0.0015$. This confirms that the layer was grown crystalline with good quality.[27] We shall note that because MB controls threading of defects and dislocations towards active region this provides varying of indium content (x) in $In_xGa_{1-x}As$ layer in wide range up to 100% (*i*-InAs). In other words by means of MB we can alter the bandgap of $In_xGa_{1-x}As$ and adjust it to optical pump 1.0–1.6 μm.

Figure 3 shows optical-pump THz-probe measurements in reflection geometry performed at room temperature with 795 nm pump for $In_{0.38}Ga_{0.62}As$ with MB. Two optical pump fluences of 45 and 580 μJ were used to excite the sample. The penetration depth of 795 nm light into $In_{0.38}Ga_{0.62}As$ is approximately 200 nm, so the 1.0 μm thickness is sufficient to absorb all of the incident pump light. As seen at later time delays, the decay of the signal can be accurately fitted by a single exponential, yielding a carrier lifetime ~ 10 ps at both optical fluences. The result is not surprising due to $In_{0.38}Ga_{0.62}As$ has good crystalline quality and thus possess much higher electron mobility in comparison to LT InGaAs. Despite this THz-TDS measurements showed that $In_{0.38}Ga_{0.62}As$ with MB provides both high THz bandwidth and intensity of THz generation. Figures 4 and 5 show THz pulse waveforms for $In_{0.38}Ga_{0.62}As$ with MB and LT GaAs in time-domain and Fourier power spectra for both samples respectively. As seen in Fig. 4 the radiation spectrum for $In_{0.38}Ga_{0.62}As$ with MB is two orders higher than for LT GaAs. This is due to much stronger intensity of THz radiation electric field in $In_{0.38}Ga_{0.62}As$ with LT MB (see Fig. 4).

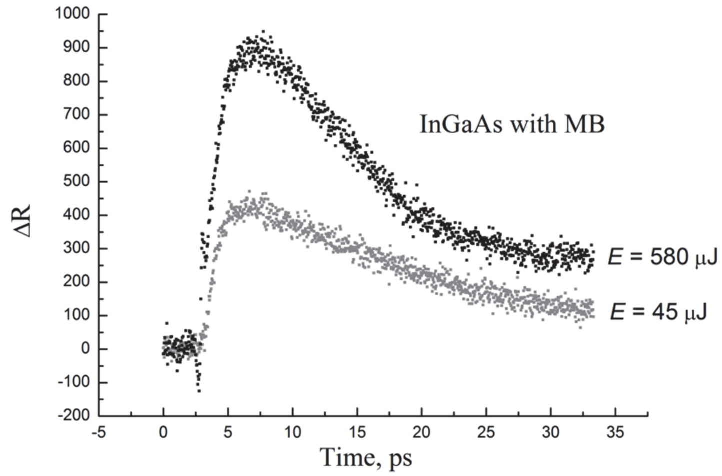

Fig. 3. Optical-pump THz-probe measurements at two pump fluences 45 and 580 μJ with 795 nm pump for $In_{0.38}Ga_{0.62}As$ with MB.

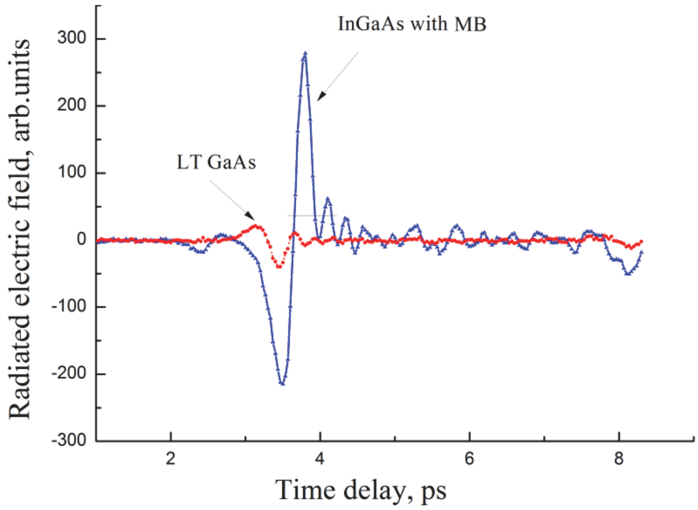

Fig. 4. THz pulse waveforms in time-domain for both samples.

It also demonstrates superior bandwidth up to 6 THz. We assume this is because of PD effect that strongly contributes to THz generation for $In_{0.38}Ga_{0.62}As$ with MB. Figure 6 indicates THz amplitude dependence on optical pump energy of Ti:S laser for $In_{0.38}Ga_{0.62}As$ with MB. The amplitude shows linear increase in log-scale with increase of pump energy. As seen at energy pump ~ 110 μJ the dependence saturates which is connected with finite density of states in $In_{0.38}Ga_{0.62}As$[28] and decrease of electron mobility due to enhanced intervalley scattering at high values of pump energy. It should be noted that for rather low optical fluence ~ 40 μJ/cm^2 the optical-to-terahertz conversion efficiency is ~ 10^{-5} that is much higher than for LT GaAs.

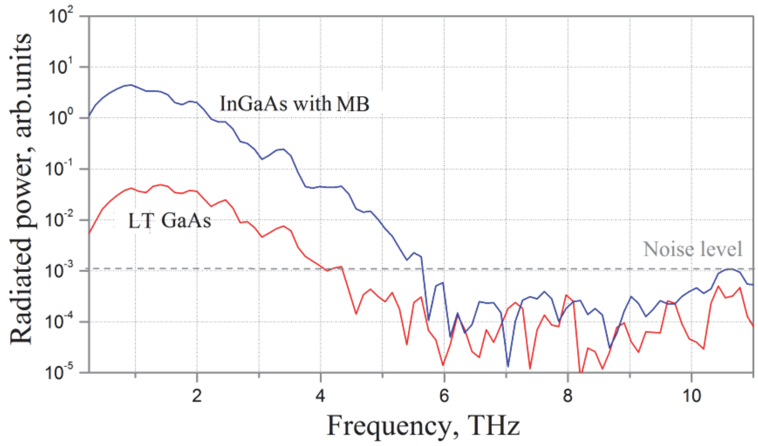

Fig. 5. Fourier power spectra for all the grown samples. Blue line indicates spectrum for InGaAs with MB, red line – for LT GaAs. Grey dotted line is system noise level.

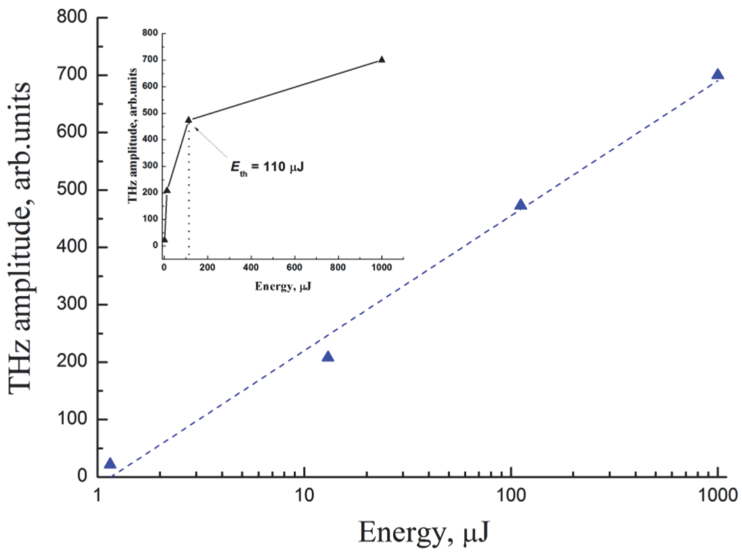

Fig. 6. THz amplitude dependence on optical excitation energy (in log-scale) for InGaAs with MB.

4. Conclusion

In conclusion, we demonstrated that $In_{0.38}Ga_{0.62}As$ photoconductive material exhibits both high THz bandwidth and optical-to-terahertz conversion efficiency and thus can be a promising candidate for use in PCA and photoconductive emitters based on lateral PD effect.[19,28] This topic will form the basis of our future work.

Acknowledgments

The work was supported by the RFBR grants № 16-32-50047, 16-07-00187 A and 16-29-03033.

References

1. C. W. Berry, N. Wang, M. R. Hashemi, M. Unlu, and M. Jarrahi, "Significant performance enhancement in photoconductive terahertz optoelectronics by incorporating plasmonic contact electrodes", *Nat. Commun.* **4** (2013) 1622.
2. R. R. Galiev, A. E. Yachmenev, A. S. Bugaev, G. B. Galiev, Yu. V. Fedorov, E. A. Klimov, R. A. Khabibullin, D. S. Ponomarev, and P. P. Maltsev, *Bul. Rus. Academ. Sci.: Phys.* **80(4)** (2016) 476–478.
3. J. T. Kindt and C. A. Schumuttenmaer, "Far-infrared dielectric properties of polar liquids probed by femtosecond terahertz pulse spectroscopy", *J. Phys. Chem.* **100(24)** (1996) 10373–10379.
4. N. T. Yardimci, S.-H. Yang, C. W. Berry, and M. Jarrahi, "High power terahertz generation using large area plasmonic photoconductive emitters", *IEEE Trans. Terahertz Sci. Technol.* **5** (2015) 223–229.
5. D. V. Lavrukhin, A. E. Yachmenev, A. S. Bugaev, G. B. Galiev, E. A. Klimov, R. A. Khabibullin, D. S. Ponomarev, and P. P. Maltsev, "Investigation of the optical properties of GaAs with δ-Si doping grown by molecular-beam epitaxy at low temperatures", *Semiconductors* **49(7)** (2015) 911–914.
6. A. Takazato, M. Kamakura, T. Matsui, J. Kitagawa, and Y. Kadoya, "Terahertz wave emission and detection using photoconductive antennas made on low-temperature-grown InGaAs with 1.56 μm pulse excitation", *Appl. Phys. Lett*., **91** (2007) 011102.
7. S.-P. Han, H. Ko, N. Kim, H.-C. Ryu, C. W. Lee, Y. A. Leem, D. Lee, M. Y. Jeon, S. K. Noh, H. S. Chun, and K. H. Park, "Optical fiber-coupled InGaAs-based terahertz time-domain spectroscopy system", *Opt. Lett*. **36(16)** (2011) 3094–3096.
8. S. Gupta, J. F. Whitaker, and G. A. Mourou, "Ultrafast carrier dynamics in III-V semiconductors grown by molecular-beam epitaxy at very low substrate temperatures", *IEEE J. Quantum Electron*. **28** (1992) 2464–2472.
9. D. C. Driscoll, M. P. Hanson, A. C. Gossard, and E. R. Brown, "Ultrafast photoresponse at 1.55 μm in InGaAs with embedded semimetallic ErAs nanoparticles", *Appl. Phys. Lett*. **86** (2005) 051908.
10. S. Preu, M. Mittendorf, H. Lu, H. B. Weber, S. Winnerl, and A.C. Gossard, "1550 nm ErAs:In(Al)GaAs large area photoconductive emitters", *Appl. Phys. Lett.* **101** (2012) 101105.
11. D. Vignaud, J. F. Lampin, E. Lefebvre, M. Zaknoune, and F. Mollot, "Electron lifetime of heavily Be-doped $In_{0.53}Ga_{0.47}As$ as a function of growth temperature and doping density", *Appl. Phys. Lett.* **80(22)** (2002) 4151.
12. N. Chimot, J. Mangeney, P. Mounaix, M. Tondusson, K. Blary, and J. F. Lampin, "Terahertz radiation generated and detected by Br^+-irradiated $In_{0.53}Ga_{0.47}As$ photoconductive antenna excited at 800 nm wavelength", *Appl. Phys. Lett*. **89** (2006) 083519.
13. M. Suzuki and M. Tonouchi, "Fe-implanted InGaAs photoconductive terahertz detectors triggered by 1.56 μm femtosecond optical pulses", *Appl. Phys. Lett*. **86** (2005) 163504.
14. V. Malevich, R. Adomavičius, and A. Krotkus, "THz emission from semiconductor surfaces", *C. R. Physique* **9** (2008) 130–141.
15. M. C. Beard, G. M. Turner, and C. A. Schmuttenmaer, "Subpicosecond carrier dynamics in low-temperature grown GaAs as measured by time-resolved terahertz spectroscopy", *J. Appl. Phys.* **90** (2001) 5915–5923.

16. A. Reklaitis, "Terahertz emission from InAs induced by photo-Dember effect: Hydrodynamic analysis and Monte Carlo simulations", *J. Appl. Phys.* **108** (2010) 053102.
17. K. Liu, J. Z. Xu, T. Yuan, and X.-C. Zhang, "Terahertz radiation from InAs induced by carrier diffusion and drift", *Phys. Rev. B* **73** (2006) 155330.
18. P. Gu, M. Tani, S. Kono, K. Sakai, and X.-C. Zhang, "Study of terahertz radiation from InAs and InSb", *J. Appl. Phys.* **91(7)** (2001) 5533.
19. G. Klatt, F. Hilser, W. Qiao, M. Beck, R. Gebs, A. Bartels, K. Huska, U. Lemmer, G. Bastian, M. B. Johnston, M. Fischer, J. Faist, and T. Dekorsy, "Terahertz emission from lateral photo-Dember currents", *Opt. Exp.* **18(5)** (2010) 4939–4947.
20. G. Matthaus, S. Nolte, R. Hohmuth, M. Voitsch, W. Richter, B. Pradarutti, S. Riehemann, G. Notni, and A. Tunnermann, "Large-area microlens emitters for powerful THz emission", *Appl. Phys. B* **96(2)** (2009) 233–235.
21. R. Singh, E. Plum, C. Menzel, C. Rockstuhl, N. Zheludev, and W. Zhang, "Negative index in chiral metamaterials", *IEEE Photonic Society 24th Annual Meeting*, Arlington, VA, USA, Oct 2011, TuG1, 240–241.
22. D. V. Lavrukhin, A. E. Yachmenev, R. R. Galiev, R. A. Khabibullin, D. S. Ponomarev, Yu. V. Fedorov, and P. P. Maltsev, "MHEMT with a power-gain cut-off frequency of f_{max} = 0.63 THz on the basis of a $In_{0.42}Al_{0.58}As/In_{0.42}Ga_{0.58}As/In_{0.42}Al_{0.58}As/GaAs$ nanoheterostructure", *Semiconductors* **48(1)** (2014) 69–72.
23. D. V. Lavrukhin, A. E. Yachmenev, R. R. Galiev, A. S. Bugaev, Y. V. Fedorov, R. A. Khabibullin, D. S. Ponomarev, and P. P. Maltsev, "Investigation and fabrication of the semiconductor devices based on metamorphic InAlAs/InGaAs/InAlAs nanoheterostructures for THz applications", *Int. J. High Speed Electron. Syst.* **24(1&2)** (2015) 1520001.
24. G. B. Galiev, R. A. Khabibullin, D. S. Ponomarev, A. E. Yachmenev, A. S. Bugaev, and P. P. Maltsev, "Metamorphic nanoheterostructures for millimeter-wave electronics", *Nanotechnol. Rus.* **10(7)** (2015) 593–599.
25. E. A. P. Prieto, S. A. B. Vizcara, A. S. Somintac, A. A. Salvador, E. S. Estacio, C. T. Que, K. Yamamoto, and M. Tani, "Terahertz emission enhancement in low-temperature-grown GaAs with an n-GaAs buffer in reflection and transmission excitation geometries", *J. Opt. Soc. Am. B* **31(2)** (2014) 291.
26. I. E. Ilyakov, G. Kh. Kitaeva, B. V. Shishkin, and R. A. Akhmedzhanov, "Terahertz time-domain electro-optic measurements by femtosecond laser pulses with an edge-cut spectrum", *Opt. Lett.* **41(13)** (2016) 2998–3001.
27. G. B. Galiev, S. S. Pushkarev, E. A. Klimov, P. P. Maltsev, R. M. Imamov, and I. A. Subbotin, "X-Ray diffractometry of metamorphic nanoheterostructures", *Cryst. Rep.* **59(2)** (2014) 258–265.
28. V. Apostolopoulos and M. E. Barnes, "THz emitters based on the photo-Dember effect", *J. Phys. D: Appl. Phys.* **47(37)** (2014) 374002.